Colloids and Surfaces B: Biointerfaces 236 (2024) 113819

Contents lists available at ScienceDirect

Colloids and Surfaces B: Biointerfaces

journal homepage: www.elsevier.com/locate/colsurfb

The mechanism of encapsulating curcumin into oleosomes (Lipid Droplets)

Umay Sevgi Vardar, Johannes H. Bitter, Constantinos V. Nikiforidis *

Biobased Chemistry and Technology, Wageningen University and Research, Bornse Weilanden 9, Wageningen 6708 WG, the Netherlands

ARTICLE INFO

Keywords:
Lipid droplets
Oil bodies
Rapeseeds
Curcumin
Lipophilic
Therapeutics

ABSTRACT

Organisms have evolved intracellular micron-sized lipid droplets to carry and protect lipids and hydrophobic minor compounds in the hydrophilic environment of cells. These droplets can be utilized as carriers of hydrophobic therapeutics by taking advantage of their biological functions. Here, we focus on the potential of plant-derived lipid droplets, known as oleosomes, as carriers for hydrophobic therapeutics, such as curcumin. By spectroscopy and confocal microscopy, we demonstrate that the oleosome membrane is permeable to hydrophobic curcumin molecules. Fluorescence recovery after photobleaching shows rapid curcumin diffusion towards oleosomes, with a diffusion time in the range of seconds. Following this, quenching probes and dilatational rheology reveal that part of the loaded curcumin molecules can accumulate at the oleosome interface, and the rest settle in the inner core. Our findings shed light on the loading mechanism of the plant-derived lipid droplets and underscore the significance of molecular localization for understanding the mechanism. This work not only enhances the understanding of the loading process but also shows potential for oleosomes use as lipid carriers.

1. Introduction

A significant number of therapeutics are insoluble in water, inhibiting their delivery into the aqueous environment of the human body [1,2]. Additionally, when hydrophobic therapeutics are exposed to human body fluids, their chemical structure might degrade due to the presence of metals and enzymes. As a result, their biological functions are being lost [3]. Therefore, hydrophobic therapeutics demand lipid-based carriers for optimal delivery and retaining therapeutics' efficacy [4,5].

Most lipid carriers are made of a mix of surfactants and polymeric molecules, which provide protection to the therapeutics [2]. However, due to their questionable toxicity and low efficiency, biocompatible and effective carriers are needed [4,5]. To overcome these limitations, employing natural lipid droplets could be a biocompatible option for therapeutic delivery.

Lipid droplets are a conserved structure in all eukaryotic organisms [6–8], composed of a triacylglycerol core surrounded by a phospholipid monolayer with embedded proteins [5,9–12]. The triacylglycerols in the lipid droplets provide energy to the cells after their hydrolysis to fatty acids. Besides triacylglycerols, lipid droplets also contain tocopherols, carotenoids, and sterols, which have biological functionality [8,13,14]. Aside from storing energy and hydrophobic molecules, lipid droplets in mammalian cells are in contact with neighboring organelles. Following the contact, they could fuel their lipid core through their phospholipid membrane to the neighboring organelles [15,16]. The minor compounds present in the lipid droplets could also be transferred together with the triacylglycerols, indicating that lipid droplets can serve as lipid carriers for hydrophobic molecules in cells [17].

Here, our research focuses on exploring the potential of the plant intracellular lipid droplets (oleosomes) as lipid carriers for hydrophobic therapeutic [1,9]. With aiming of understanding the loading mechanism and molecular localization of the therapeutics in oleosomes, curcumin was particularly chosen as a targeted therapeutic [4,5]. Curcumin is a pH-dependent tautomer molecule. It changes polarity when the pH shifts from alkaline (>8) to neutral [12,18]. In alkaline conditions, curcumin is in its hydrophilic enolic form, while at neutral and acidic conditions, curcumin is transformed into the hydrophobic keto form. Thus, by changing the pH from 12 to 7, curcumin becomes hydrophilic from hydrophobic, and it is expected to interact with the oleosomes [4,12,18]. Besides this feature, curcumin is a fluorophore which allows to investigation of its association and distribution within oleosomes using molecular probes [19]. Taken together, the pH-dependent tautomerization feature allows the loading of curcumin while the fluorescent feature lets tracking of curcumin diffusion and position into oleosomes.

Through the utilization of confocal microscopy and fluorescence quenching probes, this study tracked the loading and positioning of curcumin within oleosomes. Additionally, the interaction between curcumin and the oleosome membrane was followed using dilatational

* Corresponding author.
E-mail address: costas.nikiforidis@wur.nl (C.V. Nikiforidis).

https://doi.org/10.1016/j.colsurfb.2024.113819
Received 1 November 2023; Received in revised form 15 February 2024; Accepted 20 February 2024
Available online 27 February 2024

rheology. The findings shed light on the loading mechanism of oleosomes with hydrophobic therapeutics, suggesting their significant potential as nature-derived lipid-based carriers. The insights on the loading mechanism of oleosomes with hydrophobic therapeutics can open a new path in using cellular carriers, which are already designed by nature, for the transportation of hydrophobic molecules in the aqueous cellular environment.

2. Materials and methods

2.1. Materials

Oleosomes were extracted from untreated Alizze rapeseeds. Rapeseed oil was purchased from a local market and curcumin (purity 95%) was purchased from Alfa Aesar (UK) and all other chemicals were of analytical grade and were purchased from Sigma Aldrich (St Louis, MO, USA). The rapeseed oil used at the surface activity analysis was stripped using Florisil which was purchased from Sigma Aldrich (St Louis, MO, USA).

2.2. Oleosome extraction

Oleosomes were extracted using an alkaline aqueous buffer of NaHCO3 as was previously reported leading to a higher extraction yield of intact oleosomes [20,21]. Rapeseeds were dispersed in 0.1 M $NaHCO_3$ (pH 9.5) at a ratio of 1:7 (w/w) and kept at room temperature for 4 h under continuous magnetic stirring (VMS-C7 WVR Advanced). The dispersion was subsequently blended for 2 min at maximum speed with a kitchen blender (HR2093, Philips, Netherlands). The slurry was filtered using 2 layers of cheesecloth with a pore size of ~150 μm (GEFU®, Eslohe, Germany). The obtained filtrate was centrifuged (10, 000 g, 30 min, 4°C) (Sorvall Legend XFR, ThermoFisher Scientific, Waltham, MA, USA). After centrifugation, the cream layer was collected, and dispersed in $NaHCO_3$ (pH 9.5) at a ratio of 1:4 (w/w) and centrifuged under the same conditions as above. One more time the cream layer was collected after centrifuging and dispersed in MilliQ water at a ratio 1:4 (w/w) to purify the oleosome cream. After the final centrifugation, the cream layer was collected and stored in the fridge (4°C, overnight).

2.3. Compositional analysis

The moisture content of the oleosome cream was determined by drying the cream at 60 °C in an oven (Memmert, Memmert GmbH & Co. KG, Schwabach, Germany) until stable weight.

The oil content of the cream was determined by Soxhlet extraction with petroleum ether as a solvent. The oil content after extraction was calculated by using Eq. 1.

$$oil \quad content \quad (wt\%) = 100 * \frac{g \quad of \quad extracted \quad oil}{g \quad of \quad initial \quad sample} \tag{1}$$

The protein content of the cream was determined with the Dumas method (Rapid N exceed - N/ Protein Analyzer, Elementar). Samples, aspartic acid as a standard for the calibration curve and as control, and cellulose as a blank were combusted at a high temperature in the range of in the presence of oxygen. A nitrogen–protein conversion factor of 5.7 was used to calculate the protein content[22]. All samples were measured in duplicate.

2.4. Electrophoresis

The protein profile of the oleosome cream was determined with SDS-PAGE to determine the purity of oleosomes. Samples were run under reducing and non-reducing conditions based on the procedure described in previous work [22]. Briefly, oleosome cream was mixed with NuPAGE® LDS buffer and NuPAGE® Sample Reducing Agent for reducing condition (ThermoFisher, Landsmeer, the Netherlands). The samples and the protein marker (PageRuler™ Prestained Protein Ladder, 10–180 kDa) were loaded on a NuPAGE® Novex® 4–12% Bis-Tris Gel (ThermoFisher, Landsmeer, the Netherlands). NuPAGE® MES SDS Running Buffer (ThermoFisher, Landsmeer, the Netherlands) was added to the buffer chamber and SDS-PAGE was run for 1 hour. The gel was washed with water and stained with staining solution (Coomassie Brilliant Blue R-250 Bio-Rad Laboratories B.V., Lunteren, the Netherlands) overnight under shaking. Finally, the stained gel was washed with the de-staining solution.

2.5. Oleosome emulsion preparation and curcumin encapsulation

Oleosome cream (10 wt%) was dissolved in MilliQ water at room temperature by mixing for 1 hr. The pH-driven method was used to produce curcumin-loaded oleosomes [5], along with some modifications. Firstly, a stock alkaline curcumin solution (10 mg g^{-1}), was prepared by dissolving curcumin into sodium hydroxide solution (0.2 M, pH 12.5) in the dark at ambient temperature. To minimize the possible degradation, it was only mixed for 2 min. A known amount of curcumin alkaline solution was mixed with the oleosome emulsion, and the mixture was immediately adjusted to pH 7. The final mixture was then stirred for 5 or 10 min in the dark at ambient temperature. The final emulsion contained 0.0001 g curcumin per g oleosome cream. The curcumin-loaded oleosome emulsions were stored in the refrigerator for five days (4°C).

2.6. Encapsulation efficiency

Curcumin-loaded oleosome emulsions were centrifuged (10.000 g, 30 min). After centrifugation, the curcumin-loaded yellow cream was carefully removed from the aqueous phase. The aqueous phase was mixed with ethanol and vortexed. Free curcumin in the aqueous phase was analyzed by using UV-spectrophotometer (UV1600 PC Spectrophotometer, VWR) at 424 nm. The encapsulation efficiency was calculated by using:

$$EE = 100 * (\frac{C_{initial} - C_{unencapsulated}}{C_{initial}}) \tag{2}$$

Here EE is encapsulation efficiency, $C_{initial}$ and $C_{unencapsulated}$ are the concentrations of curcumin initially added to the system and the free curcumin measured in the aqueous phase[23]. All samples were measured in duplicate.

2.7. Microscopy

A confocal laser scanning microscope (CLSM, Leica SP8-SMD microscope, Leica Microsystems, Wetzlar, Germany) was used to visualize the microstructure of curcumin-loaded oleosome emulsion. The microscope is fitted with a 63× objective-water immersion lens. Argon ion laser and white light laser were used to image the samples. Curcumin was excited at 458 nm with Argon laser, and the emission was captured between 470 and 500 nm. Rhodamine DHPE was used to stain the phospholipid membrane was excited at 560 nm with a white light laser, and the emission was captured between 570 and 670 nm [24]. The images were captured with Leica imaging software.

During the time-point imaging analysis, the oleosome dispersion was placed on the microscope, and the pH had been pre-adjusted to 6.8. After starting the record, a few drops of an aqueous curcumin solution with a pH of 12 were added. With the addition of curcumin, no significant change in pH was observed; consequently, curcumin turned to its hydrophobic form and diffused into the oleosomes.

The fluorescence recovery after the photobleaching (FRAP) technique was used to determine the mobility of curcumin in the oleosome. The experiment was carried out with a Leica SP8-SMD microscope using a 63× water immersion lens. Samples were bleached using an argon ion

laser (100% power) at 458 nm. Image acquisition was performed using a frame size 256×256 with an 1800 Hz scan speed.

To calculate the diffusion coefficient and mobile fraction, the FRAP curves were fitted by using Eq. 3:

$$I_t = I_0 - I_1 \exp\left(-\frac{t_o}{\tau_D}\right) \quad (3)$$

here I_t is the normalized fluorescence intensity at time t, $I_0$is the recovered fluorescence at an infinite time, I_1 is the mobile fraction and τ_D is the average diffusion time.

2.8. Interfacial dilatational rheology

The interfacial dilatational rheology was investigated using an automatic drop tensiometer (ADT, Teclis TRACKER, France). A droplet, containing 0.1 wt% curcumin in stripped rapeseed oil with a surface area of 30 mm^2 was created at the tip of the needle in a cuvette filled with MilliQ water at pH 7 to determine the interfacial tension of curcumin. The stripped oil was prepared by mixing rapeseed oil with activated magnesium silicate (Florisil) in a ratio of 2:1 for 24 hrs., then centrifuged twice for 20 min at 2000 rpm and 20 °C, separating the supernatant oil each time. The interfacial tension was monitored for 2 hrs at 20 °C. During this waiting time, the droplet shape was captured with a camera, and the droplet's contour was fitted using the Young-Laplace equation to calculate the surface stress.

Further, to confirm the curcumin position at the oleosome membrane, a water droplet containing a 1 wt% oleosome solution with or without curcumin at pH 7.0 with a surface area of 30 mm^2 were created at a tip of a needle in a cuvette filled with the stripped oil. The interfacial tension of the droplet was monitored for 2 hours at 20 °C, and then oscillatory dilatational deformations were applied. A repetition of five oscillations in the area was performed at amplitudes of 5%, 10%, 15%, 20%, 30%, 40%, and 50% (at 0.02 Hz). The surface stress response was used to determine surface dilatational moduli.

2.9. Fluorescence quenching

2-bromohexadecanoic acid (2BR), 11-bromoundecanoic acid (11BR), and 16-bromohexadecanoic acid (16BR) were used as fluorescence quencher probs. These probs were incorporated into the oleosome membrane at a ratio of 15:85 (w/w) to determine the location of curcumin [19]. The molecular structures of the probes and bromine atom positions are given in Fig. 1A. In Fig. 1B, each brominated fatty acid was added into the 10% oleosome emulsion at pH 7 and then emulsions were mixed for 2 hours. After the incorporation of the fatty acids, curcumin was loaded into droplets as described above. Samples were excited at 430 nm and fluorescence emissions were recorded between 450 and 700 nm using Shimadzu RF6000 Fluorimeter. All samples were measured in duplicate.

We estimated the curcumin position by comparing the fluorescence signals of curcumin with Eq. 4:

$$\% = \left(\frac{I_Q - I_{ole}}{I_{cole} - I_{ole}}\right) x100 \quad (4)$$

Here, I_Q is curcumin fluorescence intensity in the presence of quencher prob, I_{cole} is curcumin fluorescent intensity in the absence of quencher prob and I_{ole} is oleosome fluorescent intensity.

2.10. Particle size distribution

The particle size distribution of the oleosome was determined by laser diffraction (Better sizer S3 Plus, China) after dilution of the oleo-

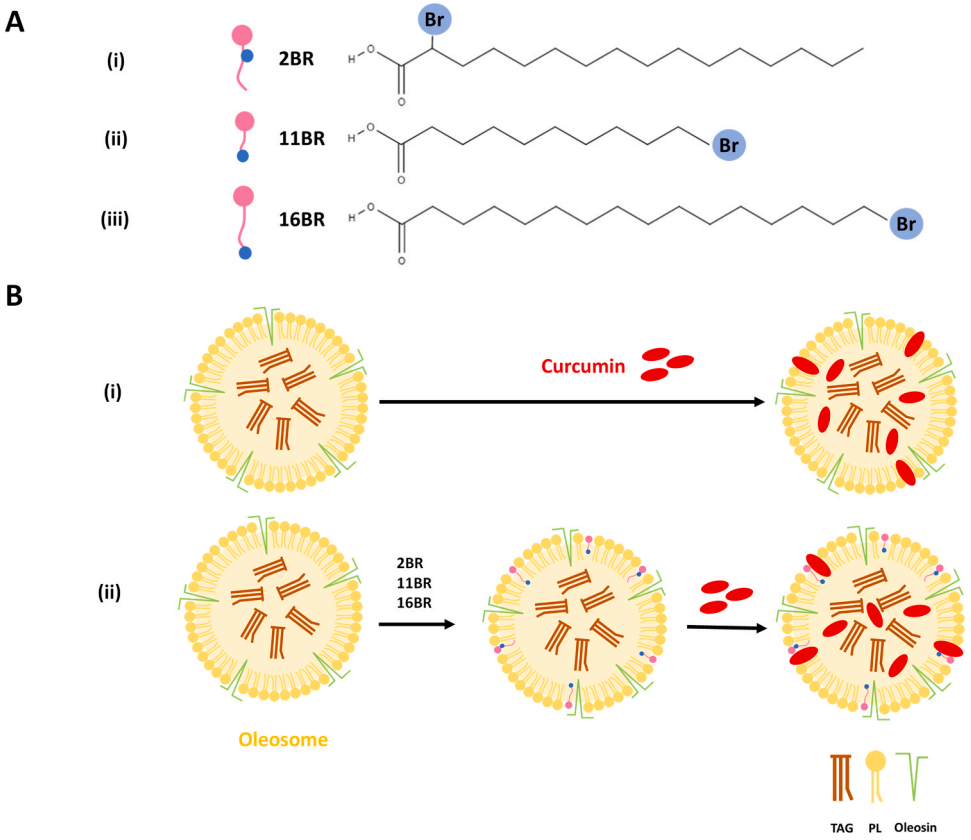

Fig. 1. A) Illustration of (i) 2BR (2-bromohexadecanoic acid), (ii) 11BR (11-bromoundecanoic acid) and (iii) 16BR (16-bromohexadecanoic acid) brominated fatty acids **B)** Schematic representation of (i) curcumin encapsulation into oleosomes, incorporation of (ii) 2BR, 11BR and 16BR probes at the oleosome membrane, and curcumin encapsulation into the oleosomes.

some emulsion and curcumin loaded-oleosome emulsions with deionized water (1:100). To investigate the presence of aggregated oleosomes and determine their actual size, 1.0 wt% sodium dodecyl sulfate [25] was added to the sample (1:1). The used refractive index was 1.47. Measurements are reported as the surface

$$d_{3,2} = \sum n_i d_i^3 \Big/ \sum n_i d_i^2 \quad (4)$$

and volume

$$d_{4,3} = \sum n_i d_i^4 \Big/ \sum n_i d_i^3 \quad (5)$$

mean diameter where n_i is the number of droplets with a diameter of d_i. All samples were measured in triplicate.

3. Results and discussion

3.1. Physicochemical characterization of extracted oleosomes

After extracting and purifying oleosomes from rapeseeds [20], their protein composition was determined both qualitatively and quantitively. The extract was a dense dispersion of oleosomes in water, containing 70.00 ±0.01 wt% triacylglycerols, 2.050 ±0.03 wt% proteins, and 27.00 ±0.01 wt% water, which was in line with values previously reported [20].

To confirm whether the oleosome extracts were pure and free of co-extracted storage proteins, we analyzed qualitatively the protein profile of the oleosome extract, using electrophoresis (SDS-PAGE). Fig. 2A provides the electropherogram of a protein marker and the proteins in the oleosome extract (lanes 1–2). It is shown that the dominant proteins present have a size of around 16–18 kDa, which is the expected size of oleosins, the main proteins present on the oleosome interface [26]. No other major protein bands belonging to co-extracted storage proteins were detected, showing that the oleosome extract was mostly free of non-oleosome related proteins.

Fig. 2B presents the oleosome particle size distribution as a volume density, which indicates that the oleosomes had a diameter from 0.8 to 5.0 μm. To confirm whether these values correspond to the diameter of individual droplets or aggregates, confocal microscopy was used (Fig. 2C), where oleosomes are shown in red. From the confocal analysis, it was shown that no aggregation took place and thus the particle sizes measured, corresponded to individual oil droplets.

3.2. Encapsulation efficiency of curcumin into oleosomes

Following the characterization of the oleosome dispersions, curcumin molecules were added into the dispersion to investigate the potential diffusion of curcumin towards the oil core of oleosomes. To achieve this, the tautomerization properties of curcumin under pH changes were exploited. Adjusting pH to 7 induces tautomerization of curcumin, and its hydrophobic keto-enolate state is formed [18,27]. As a result, curcumin can crystallize in water, or, in our case, interact with the hydrophobic patches of the surface and the core of oleosomes (Fig. 1B-i)[28,29].

By measuring the concentration of curcumin at the continuous (aqueous) phase over time we confirmed our hypothesis that curcumin diffuses towards oleosomes at pH 7. The encapsulation of curcumin took place spontaneously, with an encapsulation efficiency of 97.5±0.01 wt %. These results indicate a passive encapsulated mechanism, which takes place when a curcumin molecule is close to oleosomes and diffuses towards their core, due to hydrophobic forces[25,30,31]. Previous studies show encapsulation efficiency of 86–94 wt%, however, extraction methods and sample purity are not comparable with the stringent methods presented here.

3.3. The loading mechanism of curcumin into the oleosome

Next, we conducted a time point imaging experiment to gain further insight into the diffusion of curcumin into the surface, or the core of oleosomes. Curcumin fluorescence feature at 458 nm (shown in Fig. 3A with red) allowed us to trace it by using confocal microscopy, where curcumin, as an auto-fluorescent molecule can be easily tracked. In Figs. 3A and 3B, we show a series of sequential images over 60 sec of the diffusion of curcumin (red) into oleosomes, together with a schematic representation of curcumin diffusion.

To track oleosomes and curcumin simultaneously, we also added Rhodamine DHPE (green), which is a surface active fluorescence prob and can be co-absorbed with phospholipids at the oleosome surface[32]. Due to the focus during the recording of the video, Rhodamine DHPE could mostly be observed at the bottom left side of the images. At time zero (Fig. 3A-i), curcumin was added to the dispersion and after the pass of the first 10 sec, localization of curcumin molecules could be observed in the oleosome core (Fig. 3A-ii), indicating the rapid diffusion into the oleosome. At time intervals between 10 and 50 sec (Fig. 3A-iii/vi), the curcumin fluorescence intensity was gradually increased, indicating a further diffusion of curcumin into oleosomes. To explain the diffusion and accumulation of curcumin towards oleosomes, we schematically illustrate the mechanism in Fig. 3B.

During the passive diffusion of curcumin from the aqueous phase to the lipid phase, the molecule must interact and cross the membrane to penetrate the core. Here, although the oleosomes monolayer membrane is expected as a physical barrier for curcumin, the high encapsulation

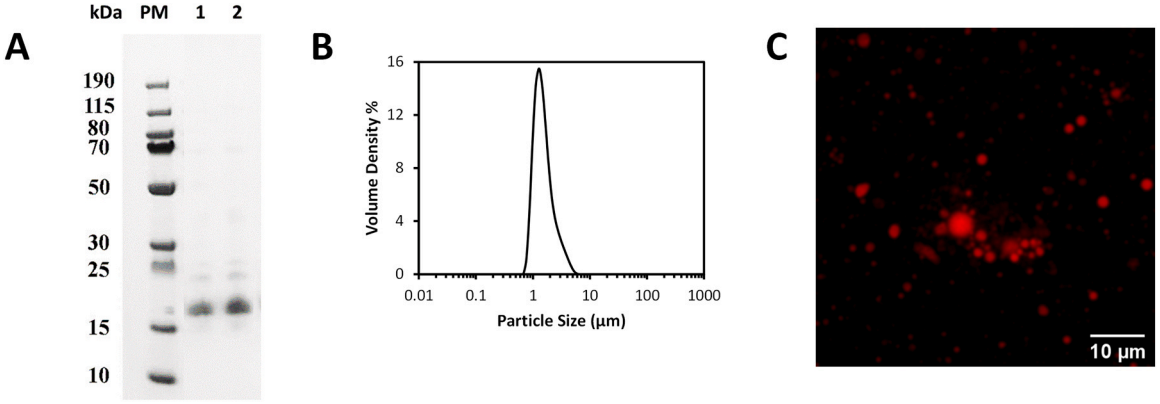

Fig. 2. A) Protein profile (SDS-PAGE) of the oleosome cream (lines 1 and 2) at reduced and non-reduced conditions and protein marker (PM) **B)** Individual particle size distribution as a percentage of volume density of 10 wt% oleosome emulsions after the addition of 1.0 wt% SDS. **C)** CLSM image of the oleosome shown in red stained with Nile red. Scale bar at the bottom right (10 μm).

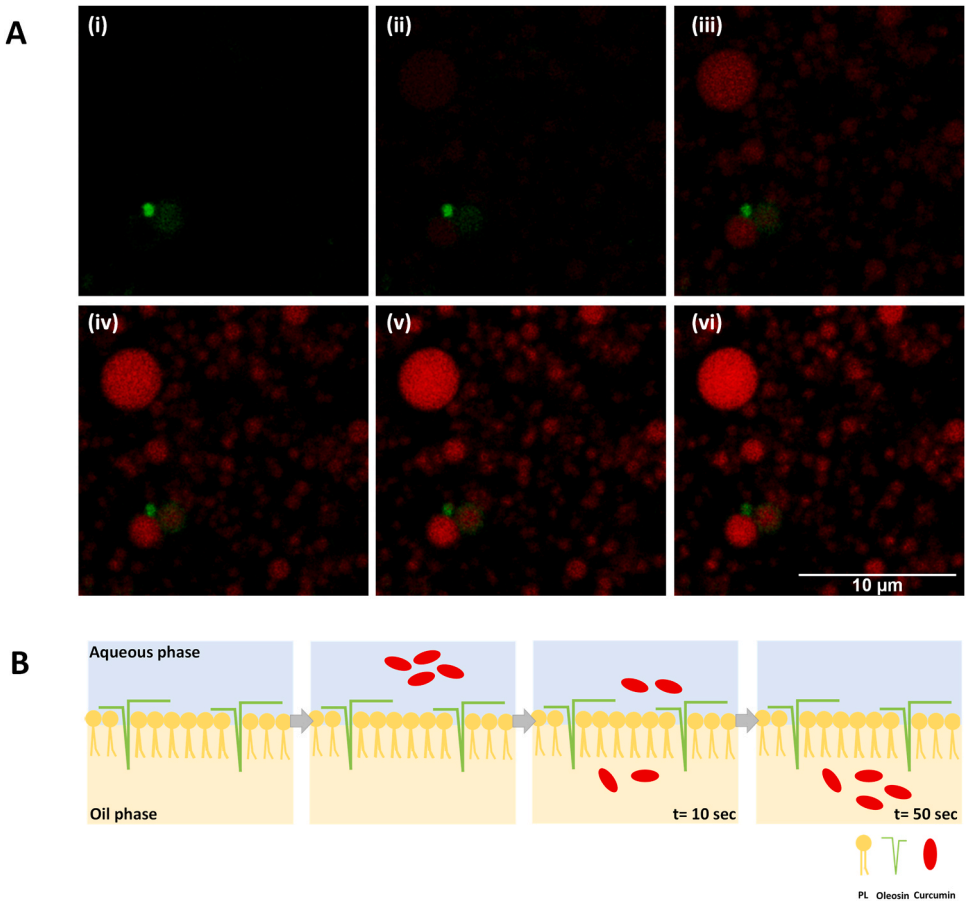

Fig. 3. A) The confocal microscopy image series of curcumin encapsulation during 50ss, curcumin, and Rhodamine DHPE are shown with red and green, respectively. The scale bar is bottom right. **B)** illustration of curcumin diffusion from the aqueous phase to oleosome triacylglycerol core based on pH-dependent curcumin hydrophobicity.

rate and rapid diffusion of curcumin proved that the membrane does not act as a barrier for curcumin. Previously, molecular dynamic simulations confirmed packing defects on the oleosome membrane, these defects allow the binding of proteins at the oleosomes membrane in the cell [33, 34]. Similarly, fluorescently labeled phospholipids can also attach oleosome membrane, indicating voids of the oleosome membrane [35–37]. We, therefore, hypothesize that the diffusion of curcumin into oleosomes takes place when the hydrophobic curcumin molecules are in the proximity of the oleosome interface voids and attractive hydrophobic forces take place.

With the time point experiment, we showed that the diffusion of curcumin takes place mostly in the first 20 s and the fluorescent intensity rapidly increased in the first few seconds. To make the initial rapid diffusion curcumin clear, we performed an additional experiment and took advantage of fluorescence recovery after photobleaching (FRAP). Initially, intense laser light was used to bleach curcumin fluorescence in the selected region, and this was taken as the t_0. The diffusion of curcumin into the bleached area directly after the photobleaching moment was monitored and the fluorescence recovery of curcumin in that area was recorded.

The outcome of the FRAP analysis is a plot of the recovery of the curcumin fluorescence intensity ratio with time, as is given in Fig. 4. The diffusion of curcumin in the core of the bleached oleosomes started immediately after the bleaching step, reaching equilibrium at 10 sec [38,39]. The obtained curve was fitted according to Eq. (3) and the average diffusion time (τ_D) was calculated as the needed time for the curcumin intensity recovery. Shorter diffusion time indicates a more rapid diffusion. In our system, the fluorescence intensity of curcumin was recovered up to 50% in 1.325 sec and reached a maximum of 66% in

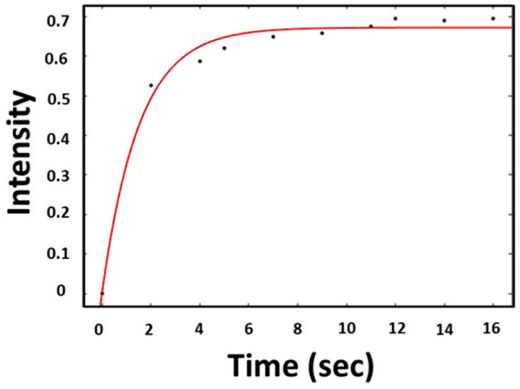

Fig. 4. Time-dependent fluorescence intensity of curcumin into oleosome after photobleaching.

10 sec. The results confirmed the microscopy images in Fig. 3A, where 50% of the available curcumin diffused in the oil phase in 2 sec, and between 10 and 20 sec a plateau in fluorescent intensity was reached.

3.4. *Interactions of curcumin with the oleosome interface*

Confocal microscopy images of loaded oleosomes showed that curcumin is able to diffuse into the oleosome core. However, curcumin molecules contain both polar and apolar domains which might make them surface active. This would mean that curcumin could participate at

the oleosome membrane, which is an oil-water interface. To investigate this hypothesis, we initially measured the curcumin interfacial activity and we found that curcumin molecules adsorb on a pure oil-water interface and reduce the interfacial tension from ~26 mN/m to ~14 mN/m and reach an equilibrium after 120 mins.

To further investigate the participation of curcumin on the oleosome interface, we used the oleosome interfacial membrane and measures its dilatational viscoelastic properties with and without the presence of curcumin. In Fig. 5, we show the dilatational elastic (Ed') and viscous (Ed") moduli of an oil-water interface stabilized by the oleosome interfacial membrane, with or without the presence of curcumin. The film made using the oleosome membrane, showed decreasing elastic moduli from 17 mN/m at 5% deformation to 11 mN/m at 50% deformation, while the curcumin-loaded oleosome film showed decreasing elastic moduli from 24 mN/m at 5% deformation to 17 mN/m at 50% deformation. Overall, the elastic moduli of curcumin-loaded oleosomes were higher than the moduli of oleosomes at all deformations, indicating that curcumin participates in the interface and plays an interactive role between the phospholipids and proteins.

3.5. Quenching probes to track the positioning of curcumin into oleosomes

We have shown that curcumin, besides going into the hydrophobic core of oleosomes, it also participates in the oleosome interfacial membrane. However, the exact positioning on the interface is not clear and is crucial to understand since it can affect the physicochemical properties of oleosomes and the release mechanism of curcumin.

Curcumin, therefore, could be located in one of the three main areas of oleosomes with different molecular compositions: i) the triacylglyceride (TAG) core, ii) the hydrophilic outer surface, which is comprised of the hydrophilic protein termini and the polar heads of phospholipids, and iii) the area of the fatty acids of the phospholipid which are loosely aligned together. We, therefore, focused on the second and third hypotheses in this section to determine the exact position of curcumin at the membrane.

To gain deeper insight into the distribution of curcumin molecules in the oleosome structure, we conducted fluorescence quenching analysis by using quenching probes [19,40,41]. The fluorescence quenching probes are based on the incorporation of a heavy atom in the system, which leads to a strong decrease in the fluorescence intensity through an effect on the energy state of the electrons [42]. To identify whether the fluorescence sites of the absorbed curcumin are located next to the phospholipid heads, next to the fatty acids of the phospholipids, or in the TAG core, we used three specific brominated fatty acids as fluorescence probes. The surface-active nature of the probes allows them to be adsorbed on phospholipid bilayers [19,41]. Similarly, this behavior is expected for phospholipid monolayers, as previously mentioned with fluorescently labeled phospholipids [35] and surfactants [43] at the oleosome interface.

The brominated fatty acids used had a bromide at a position next to the polar carboxyl group or in the middle of the fatty acid chain or at the end of the fatty acid chain. Having a bromide at different positions could allow collecting information at different depths of the membrane by measuring the effect on the fluorescence decrease of the curcumin molecule. In particular, a C11 fatty acid with the bromide at the C2 position (2-bromohexadecanoic acid (2BR) (Fig. 1A-i) was added to quench the fluorescence of the curcumin molecules that could be adsorbed on the surface. A C11 fatty acid with the bromide at the C11 position (11-bromoundecanoic acid (11BR)) (Fig. 1A-ii) was added to quench the curcumin molecules that prefer to sit with the fatty acids of the phospholipids, and a C16 fatty acid with the bromide at the C16 position (16-bromo-hexadecanoic acid (16BR)) (Fig. 1A-iii) was added to quench curcumin molecules that are on the interface of the phospholipid tails and the triacylglycerols.

The changes in the emission spectra of the samples (curcumin-loaded oleosomes) without any brominated acid and with the three types of brominated fatty acids are given in Fig. 6. In the absence of curcumin, oleosomes have no fluorescence (Figure S1). Overall, upon adding each of the three brominated fatty acids derivatives, the fluorescence intensity of curcumin was decreased compared to the absence of brominated fatty acids. The fluorescence intensity of the curcumin-loaded oleosomes was initially at 100385. When the bromide was added next to the head of the phospholipids, the fluorescence intensity decreased to 91588. When the bromide was added in the middle of the phospholipid fatty acids and added at the interface of the phospholipid fatty acids and triacylglycerols, the fluorescence intensity decreased to 97849 and 95523, respectively. The decreases in fluorescence after the addition of a bromine atom indicate that curcumin does not exclusively sit in the liquid triacylglycerol core, and they can lie on phospholipids' heads and/or co-adsorb with the phospholipids. Thus, curcumin might locate in all hypothesized locations, but primarily in the core.

Curcumin molecules are adsorbed on the interface due to their interfacial activity and also due to the hydrophobic attractive interactions with the phospholipid fatty acids and proteins, showing that the interface of oleosomes is not fully saturated. The higher decrease in fluorescence intensity when the 2BR and the 16BR were used, indicates that the curcumin is probably interacting with the phospholipid head or absorbed parallelly or vertically to the phospholipid fatty acids. Although we can estimate the curcumin position based on the decrease in fluorescence, the estimation might not be straightforward due to the similarity of curcumin molecule length (~1.6 nm) and the length of brominated fatty acids. If curcumin lies on the interface, the fluorescence intensity of curcumin might be quenched by only 2BR; however, if

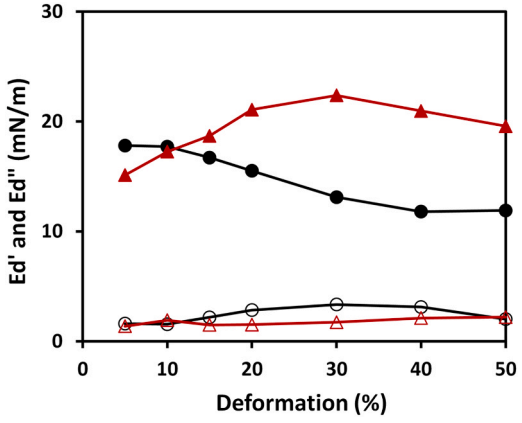

Fig. 5. Dilatational elastic modulus (Ed': filled symbol) and viscous modulus (Ed'': hollow symbol) over deformation amplitude of oleosome (black, ○), and curcumin-loaded oleosome (red, Δ) at a constant frequency of 0.02 Hz.

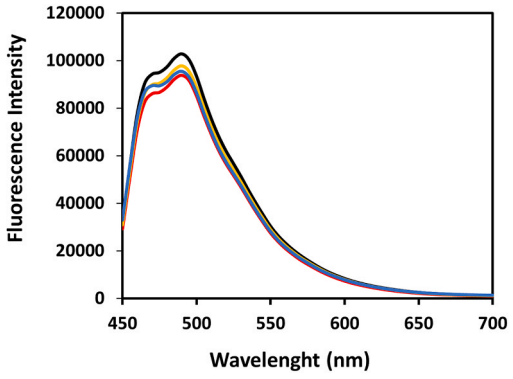

Fig. 6. Fluorescence emission spectra of curcumin-loaded oleosomes in the absence of fatty acids (black line), in the presence of 2BR (2-bromohexadecanoic acid) (red line), 11BR (11-bromoundecanoic acid) (yellow line), 16BR (16-bromohexadecanoic acid) (blue line) fatty acids.

curcumin is parallelly adsorbed in the membrane, curcumin fluorescence might be quenched by all brominated fatty acids no matter where the bromine is e.g. when an aromatic ring of curcumin is near the 2BR, the other aromatic ring would be near the 16BR.

3.6. Physicochemical stability of oleosomes during storage after the adsorption of curcumin

The presence of curcumin at the oleosome interface could affect their physical stability, therefore we measured the size distribution of oleosomes before and after the curcumin encapsulation and during five days storage at 4 °C. Fig. 7A and B show the volume-based droplet size distribution of individual oleosomes. Regardless of the presence of curcumin, we observed a monomodal size distribution (Fig. 7A) with an average size distribution ($d_{4,3}$) at 1.4±0.02 for fresh oleosomes. After five days of storage, oleosomes with or without curcumin continued to show monomodal size distribution (Fig. 7B), showing that curcumin did not affect the oleosome stability.

Besides light scattering, confocal microscopy was also used to confirm the size of curcumin-loaded oleosomes. The micrographs are displayed in Fig. 7C and D, and it was confirmed that oleosomes (shown as red) had a diameter smaller than 2 μm, and their particle size did not change during storage. Additionally, we do not expect a significant impact of the pH shifting from 9 to 7 on oleosomes structure due to the similar negative charge at both pHs, which was proven by previously published works [35].

4. Conclusion

We showed that when curcumin molecules were dispersed in an oleosome dispersion and transformed into their hydrophobic keto form, they spontaneously (about 95% when using 0.0001 g curcumin per g of oleosome) diffused into oleosomes most likely due to hydrophobic forces. Using confocal microscopy and the fluorescent recovery after the photobleaching (FRAP) technique, it was found that curcumin diffused in 10 seconds into oleosomes, and the fluorescent intensity reached a plateau in 5 sec. Our bromide fluorescence quenching probes showed that a part of the curcumin molecules remain at the oleosome interface, while the rest of the curcumin is located in the oleosome triacylglycerol core. Finally, the presence of added curcumin at the interface does not alter the physical stability of oleosomes during storage. Considering these results, we anticipate that this study will contribute to a better understanding of the hydrophobic molecules' entrance into the oleosomes. Through our findings we clearly show that hydrophobic molecules such as curcumin can be encapsulated in oleosomes, proving that oleosomes can serve as carriers of lipophilic therapeutics.

CRediT authorship contribution statement

Umay Sevgi Vardar: Conceptualization, Data curation, Formal analysis, Funding acquisition, Investigation, Methodology, Validation, Visualization, Writing – original draft. **Johannes H. Bitter:** Supervision, Writing – review & editing. **Costas Nikiforidis:** Conceptualization, Project administration, Supervision, Writing – review & editing.

Declaration of Competing Interest

The authors declare that they have no known competing financial interests or personal relationships that could have appeared to influence the work reported in this paper.

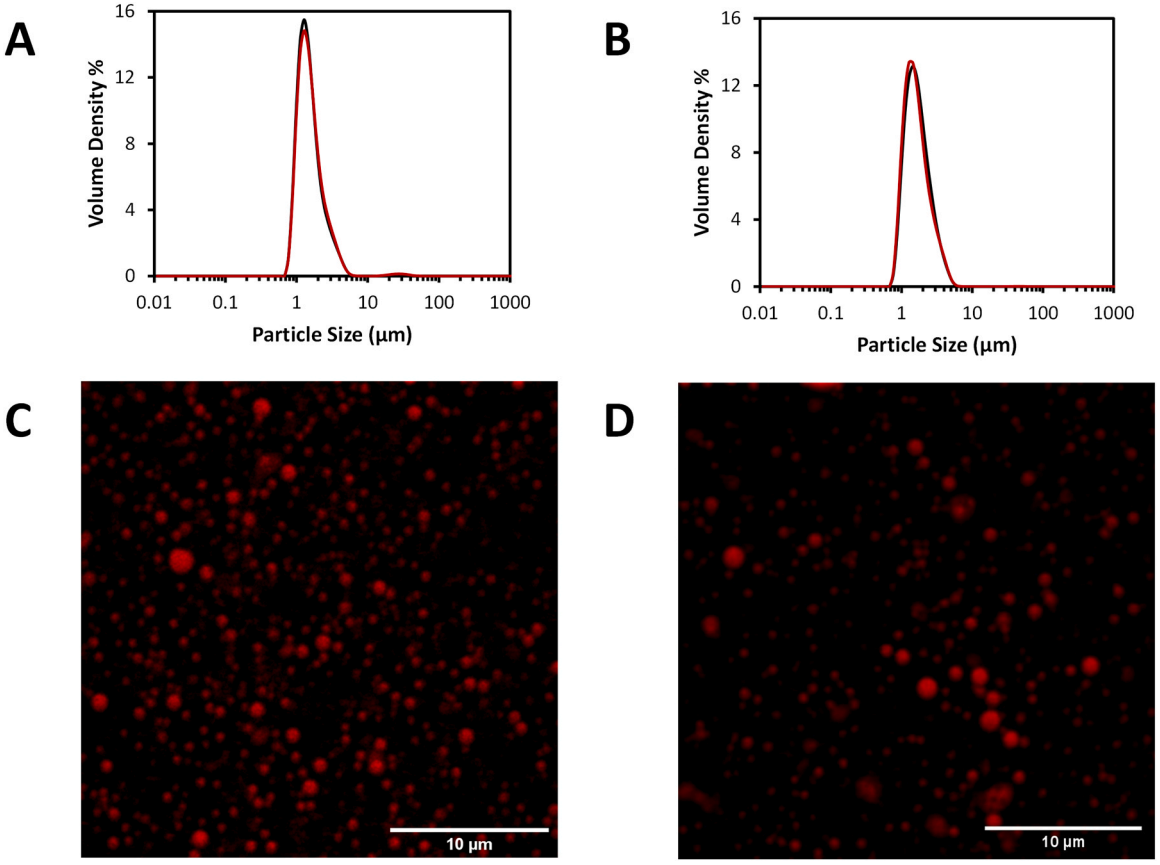

Fig. 7. The individual oleosome particle size distribution as a percentage of volume density **A)** fresh **B)** after five days storage at pH 7 (black line) and curcumin loaded oleosome at pH 7 (red line) after addition of 1.0 wt% sodium dodecyl sulfate. CLSM images of the curcumin-loaded oleosome emulsions at pH 7 **C)** fresh and **D)** after five days storage. Curcumin is shown with red color and the scale bar is bottom right.

Data availability

Data will be made available on request.

Funding

This work was supported by the Ministry of National Education in the Republic of Türkiye.

Appendix A. Supporting information

Supplementary data associated with this article can be found in the online version at doi:10.1016/j.colsurfb.2024.113819.

References

[1] A. Acevedo-Fani, A. Dave, H. Singh, Nature-assembled structures for delivery of bioactive compounds and their potential in functional foods, Front. Chem. 8 (2020) 564021.
[2] M. Kharat, D.J. McClements, Recent advances in colloidal delivery systems for nutraceuticals: a case study – delivery by design of curcumin, J. Colloid Interface Sci. 557 (2019) 506–518.
[3] H.-Y. Cho, T. Lee, J. Yoon, Z. Han, H. Rabie, K.-B. Lee, W.W. Su, J.-W. Choi, Magnetic oleosome as a functional lipophilic drug carrier for cancer therapy, ACS Appl. Mater. Interfaces 10 (2018) 9301–9309.
[4] A. Araiza-Calahorra, M. Akhtar, A. Sarkar, Recent advances in emulsion-based delivery approaches for curcumin: from encapsulation to bioaccessibility, Trends Food Sci. Technol. 71 (2018) 155–169.
[5] B. Zheng, X. Zhang, S. Peng, D.J. McClements, Impact of curcumin delivery system format on bioaccessibility: nanocrystals, nanoemulsion droplets, and natural oil bodies, Food Funct. 10 (2019) 4339–4349.
[6] D.J. Murphy, The dynamic roles of intracellular lipid droplets: from archaea to mammals, Protoplasma 249 (2012) 541–585.
[7] T.C. Walther, R.V. Farese Jr, Lipid droplets and cellular lipid metabolism, Annu. Rev. Biochem. 81 (2012) 687.
[8] M.A. Welte, A.P. Gould, Lipid droplet functions beyond energy storage, Biochim. Biophys. Acta (BBA)-Mol. Cell Biol. Lipids 1862 (2017) 1260–1272.
[9] C.V. Nikiforidis, Structure and functions of oleosomes (oil bodies), Adv. Colloid Interface Sci. 274 (2019) 102039.
[10] I.D. Fisk, R. Linforth, G. Trophardy, D. Gray, Entrapment of a volatile lipophilic aroma compound (d-limonene) in spray dried water-washed oil bodies naturally derived from sunflower seeds (Helianthus annus), Food Res. Int. 54 (2013) 861–866.
[11] C. Nikiforidis, V. Kiosseoglou, E. Scholten, Oil bodies: an insight on their microstructure—maize germ vs sunflower seed, Food Res. Int. 52 (2013) 136–141.
[12] B. Zheng, X. Zhang, H. Lin, D.J. McClements, Loading natural emulsions with nutraceuticals using the pH-driven method: formation & stability of curcumin-loaded soybean oil bodies, Food Funct. 10 (2019) 5473–5484.
[13] Z. Papackova, M. Cahova, Fatty acid signaling: the new function of intracellular lipases, Int. J. Mol. Sci. 16 (2015) 3831–3855.
[14] W.-J. Shen, S. Azhar, F.B. Kraemer, Lipid droplets and steroidogenic cells, Exp. Cell Res. 340 (2016) 209–214.
[15] A.R. Thiam, E. Ikonen, Lipid droplet nucleation, Trends Cell Biol. 31 (2021) 108–118.
[16] J.A. Olzmann, P. Carvalho, Dynamics and functions of lipid droplets, Nat. Rev. Mol. Cell Biol. 20 (2019) 137–155.
[17] A.R. Thiam, R.V. Farese Jr, T.C. Walther, The biophysics and cell biology of lipid droplets, Nat. Rev. Mol. Cell Biol. 14 (2013) 775–786.
[18] R. Jagannathan, P.M. Abraham, P. Poddar, Temperature-dependent spectroscopic evidences of curcumin in aqueous medium: a mechanistic study of its solubility and stability, J. Phys. Chem. B 116 (2012) 14533–14540.
[19] A. Karewicz, D. Bielska, B. Gzyl-Malcher, M. Kepczynski, R. Lach, M. Nowakowska, Interaction of curcumin with lipid monolayers and liposomal bilayers, Colloids Surf. B: Biointerfaces 88 (2011) 231–239.
[20] M.J. Romero-Guzmán, N. Köllmann, L. Zhang, R.M. Boom, C.V. Nikiforidis, Controlled oleosome extraction to produce a plant-based mayonnaise-like emulsion using solely rapeseed seeds, Lwt 123 (2020) 109120.
[21] S. De Chirico, V. di Bari, T. Foster, D. Gray, Enhancing the recovery of oilseed rape seed oil bodies (oleosomes) using bicarbonate-based soaking and grinding media, Food Chem. 241 (2018) 419–426.
[22] E. Ntone, J.H. Bitter, C.V. Nikiforidis, Not sequentially but simultaneously: Facile extraction of proteins and oleosomes from oilseeds, Food Hydrocoll. 102 (2020) 105598.
[23] S. Peng, Z. Li, L. Zou, W. Liu, C. Liu, D.J. McClements, Enhancement of curcumin bioavailability by encapsulation in sophorolipid-coated nanoparticles: an in vitro and in vivo study, J. Agric. Food Chem. 66 (2018) 1488–1497.
[24] Y. Song, N. Zhang, Q. Li, J. Chen, Q. Wang, H. Yang, H. Tan, J. Gao, Z. Dong, Z. Pang, Z. Huang, J. Qian, J. Ge, Biomimetic liposomes hybrid with platelet membranes for targeted therapy of atherosclerosis, Chem. Eng. J. 408 (2021) 127296.
[25] S. Dimitrov, N. Dimitrova, J. Walker, G. Veith, O. Mekenyan, Predicting bioconcentration factors of highly hydrophobic chemicals. Effects of molecular size, Pure Appl. Chem. 74 (2002) 1823–1830.
[26] J.T. Tzen, Integral proteins in plant oil bodies, Int. Sch. Res. Not. 2012 (2012).
[27] N.K. Bhatia, S. Kishor, N. Katyal, P. Gogoi, P. Narang, S. Deep, Effect of pH and temperature on conformational equilibria and aggregation behaviour of curcumin in aqueous binary mixtures of ethanol, RSC Adv. 6 (2016) 103275–103288.
[28] M.N. Oskouie, N.S. Aghili Moghaddam, A.E. Butler, P. Zamani, A. Sahebkar, Therapeutic use of curcumin-encapsulated and curcumin-primed exosomes, J. Cell. Physiol. 234 (2019) 8182–8191.
[29] E.I. Paramera, S.J. Konteles, V.T. Karathanos, Microencapsulation of curcumin in cells of Saccharomyces cerevisiae, Food Chem. 125 (2011) 892–902.
[30] L.R. De Young, K.A. Dill, Solute partitioning into lipid bilayer membranes, Biochemistry 27 (1988) 5281–5289.
[31] F. Acevedo, M. Rubilar, I. Jofré, M. Villarroel, P. Navarrete, M. Esparza, F. Romero, E.A. Vilches, V. Acevedo, C. Shene, Oil bodies as a potential microencapsulation carrier for astaxanthin stabilisation and safe delivery, J. Microencapsul. 31 (2014) 488–500.
[32] B. Chazotte, Labeling membranes with fluorescent phosphatidylethanolamine, Cold Spring Harb. Protoc. 2011 (2011) pdb. prot5621.
[33] C. Prevost, M.E. Sharp, N. Kory, Q. Lin, G.A. Voth, R.V. Farese, Jr, T.C. Walther, Mechanism and determinants of amphipathic helix-containing protein targeting to lipid droplets, Dev. Cell 44 (2018), 73-86 e74.
[34] A. Bacle, R. Gautier, C.L. Jackson, P.F.J. Fuchs, S. Vanni, Interdigitation between triglycerides and lipids modulates surface properties of lipid droplets, Biophys. J. 112 (2017) 1417–1430.
[35] Z. Ma, J.H. Bitter, R.M. Boom, C.V. Nikiforidis, Thermal treatment improves the physical stability of hemp seed oleosomes during storage, LWT 189 (2023) 115551.
[36] Y. Gao, Y. Zheng, F. Yao, F. Chen, Effects of pH and temperature on the stability of peanut oil bodies: new insights for embedding active ingredients, Colloids Surf. A: Physicochem. Eng. Asp. 654 (2022) 130110.
[37] E. Ntone, B. Rosenbaum, S. Sridharan, S.B.J. Willems, O.A. Moultos, T.J.H. Vlugt, M.B.J. Meinders, L.M.C. Sagis, J.H. Bitter, C.V. Nikiforidis, The dilatable membrane of oleosomes (lipid droplets) allows their in vitro resizing and triggered release of lipids, Soft Matter 19 (2023) 6355–6367.
[38] D. Blumenthal, L. Goldstien, M. Edidin, L.A. Gheber, Universal approach to FRAP analysis of arbitrary bleaching patterns, Sci. Rep. 5 (2015) 1–9.
[39] T.K. Meyvis, S.C. De Smedt, P. Van Oostveldt, J. Demeester, Fluorescence recovery after photobleaching: a versatile tool for mobility and interaction measurements in pharmaceutical research, Pharm. Res. 16 (1999) 1153–1162.
[40] A. Ausili, V. Gómez-Murcia, A.M. Candel, A. Beltrán, A. Torrecillas, L. He, Y. Jiang, S. Zhang, J.A. Teruel, J.C. Gómez-Fernández, A comparison of the location in membranes of curcumin and curcumin-derived bivalent compounds with potential neuroprotective capacity for Alzheimer's disease, Colloids Surf. B: Biointerfaces 199 (2021) 111525.
[41] E. El Khoury, D. Patra, Length of hydrocarbon chain influences location of curcumin in liposomes: curcumin as a molecular probe to study ethanol induced interdigitation of liposomes, J. Photochem. Photobiol. B: Biol. 158 (2016) 49–54.
[42] D. Ke, X. Wang, Q. Yang, Y. Niu, S. Chai, Z. Chen, X. An, W. Shen, Spectrometric study on the interaction of dodecyltrimethylammonium bromide with curcumin, Langmuir 27 (2011) 14112–14117.
[43] C.V. Nikiforidis, V. Kiosseoglou, Competitive displacement of oil body surface proteins by Tween 80–Effect on physical stability, Food Hydrocolloids 25 (5) (2011) 1063–1068.